

Structure of atomically perfect lines of bismuth in the Si(001) surface

D. R. Bowler*

Department of Physics and Astronomy, University College London, Gower Street, London WC1E 6BT, United Kingdom

(Received 19 April 2000)

Atomically perfect lines of bismuth (200 nm long or more) form in the Si(001) surface when a bismuth covered surface is annealed around the bismuth desorption temperature. We describe modeling results for the structure of these lines based on tight binding calculations, examine evidence for their extraordinary perfection, and describe the procedure used to fit the tight binding parametrization. The perfection of the lines is found to arise from a combination of thermodynamic and kinetic reasons.

I. INTRODUCTION

As the quest for nanotechnology, and electronics on the nanoscale, is pursued, one-dimensional systems that might act as quantum wires are of great interest, but are rather difficult to prepare experimentally. The *spontaneous* formation of lines of bismuth several hundred nanometers long without kink or defect has been reported;^{1,2} while the electronic properties of these features (referred to as ‘‘nanolines’’ given their size) are not ideal for use as wires, their extraordinary perfection offers the best prospect of actually constructing real quantum wires yet seen. Understanding their atomic and electronic structure is of great importance.

Bismuth is used as a surfactant (an alternative to arsenic or antimony^{3,4}) during Si or Ge growth on Si(001) or Ge(001).⁵ At room temperature, it initially adsorbs as adatoms on the Si(001) dimer rows, which then pair up to form dimers, perpendicular to the underlying dimers, and on top of the Si(001) dimer rows.^{6,7} This leads to a (1×2) reconstruction,^{6,8-11} which develops into a (2×2) reconstruction as the dimers line up across the rows.^{6,10,11} Eventually, a strain-induced $(2 \times n)$ reconstruction is seen.^{7,12}

Under certain circumstances bismuth will form long, perfectly straight lines embedded in the Si(001) surface.^{1,2} Two separate recipes have been found for their formation: dosing the Si(001) surface with Bi at a low temperature, followed by heating briefly to the desorption temperature; or, alternatively, exposing the Si(001) surface to Bi around the desorption temperature. Under both these preparation conditions, perfectly straight, atomically perfect lines form in the Si(001) surface, each up to several hundred nanometers long, and often terminated in a pair of three-missing-dimer defects (2×3 DV's). This is illustrated in Fig. 1. A more detailed examination of the scanning tunneling microscopy (STM) data^{1,2} reveals that the nanolines have a larger band gap than the surrounding Si(001) surface; this means that they may not be useful in their present state as one-dimensional conductors, but might be useful as templates for nanowires; alternatively, an understanding of their formation mechanism might allow the substitution of another element for bismuth to yield better electronic properties.

An investigation of such a system is ideal for close collaboration between experiment and theory; while STM images can give much information about the appearance of surface features, and atomistic modeling can give details of

energetics of various structures, often only the combination of the two (as described recently in some detail¹³) will conclusively identify structures and growth mechanisms. The results of such a collaboration on the structure of the lines have been presented elsewhere;^{1,2} here the theoretical details are presented and the structure and perfection of the lines are examined. The computational details are given in the next section, followed by sections describing the structure of the lines and their perfection, and finally the conclusion. Details of the tight binding parametrization created to model Si-Bi and Bi-Bi bonds and tests of its validity are given in the Appendixes.

II. COMPUTATIONAL DETAILS

In order to model the atomic and electronic structure of the lines, which involve Si and Bi (which are, respectively, a semiconductor and a semimetal in their elemental forms), a method using quantum mechanics was clearly required.

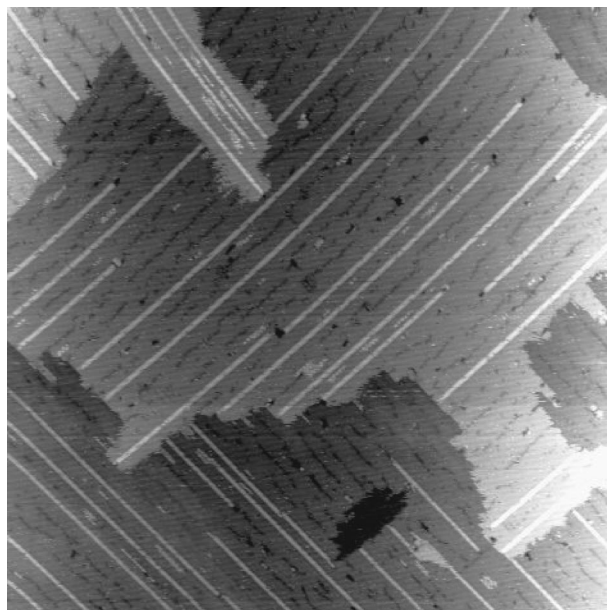


FIG. 1. A STM image, $200 \times 200 \text{ nm}^2$, showing the bismuth lines in a Si(001) surface. The lines are perfectly straight and show no defects. Any curvature is due to STM drift. Bias voltage was +2.0 V. *Courtesy of Dr. K. Miki.*

However, the unit cells required to investigate the kinking and perfection of the lines are large (up to several thousand atoms to isolate kinks and defects), ruling out *ab initio* electronic structure techniques (which are limited to a few hundred atoms). Tight binding provides a good compromise between the two requirements of quantum mechanical accuracy and computational efficiency.¹⁴

Tight binding postulates (and in some cases specifies) a basis set of local, atomiclike orbitals. The Hamiltonian is written in terms of matrix elements between these orbitals, which are then parametrized, generally being written as an equilibrium hopping integral multiplied by a scaling term. Cohesive energies are obtained by adding a pairwise repulsive term; the whole procedure has been rather elegantly justified by Sutton *et al.*¹⁵ Details of the parametrization for Si-Si bonds (and Si-H bonds which are used to terminate the base of the slab) are given elsewhere,¹⁶ while the details of the Bi-Si and Bi-Bi bonds are given in Appendix A. The parametrization was tested by calculating the energies for a bismuth dimer in various sites on the Si(001) surface, and comparing these with *ab initio* calculations. This is described in Appendix B.

As the computational cells were all rather large (a minimum size of 200 atoms, extending up to 1600 atoms), a tight binding technique for which the computational effort scaled linearly with the number of atoms was used¹⁷ (an implementation¹⁸ of the density matrix method¹⁹). In a recent comparison of methods,²⁰ the density matrix method was found to be the most efficient and accurate for semiconductors, particularly when there were states in the gap (e.g., at a semiconductor surface).

The unit cells were constructed to ensure adequate isolation within periodic supercells. All unit cells were ten layers of silicon deep, with the bottom five layers held fixed in bulklike positions and the final layer terminated in hydrogen. The cells were eight dimers long, which resulted in a separation of five dimers between successive nanolines. The larger unit cells used for calculating termination separated images by three silicon dimer rows; these cells contained up to 1600 atoms, which tested (and vindicated) the use and applicability of linear scaling methods.

As this is a mixed system, the question of how to compare energies between structures with different numbers of silicon and bismuth atoms arises. The approach chosen here is to calculate the excess surface energy plus bismuth adsorption energy per dimer for each structure. The chemical potential used for silicon is the bulk (diamond structure) energy, and the surface energy for a silicon slab of the same area is used to give excess surface energy; as the system modeled has contact with what is, in effect, a vast reservoir of bulk silicon, this seems like an appropriate choice.

III. STRUCTURE OF THE BISMUTH LINES

In this section, the detailed atomic model for the bismuth nanoline will be considered, along with the questions of termination and perfection of these lines.

A. Atomic model for the line

The structure of these lines as seen in STM is rather intriguing, and shown in closeup in Fig. 2. The lines run per-

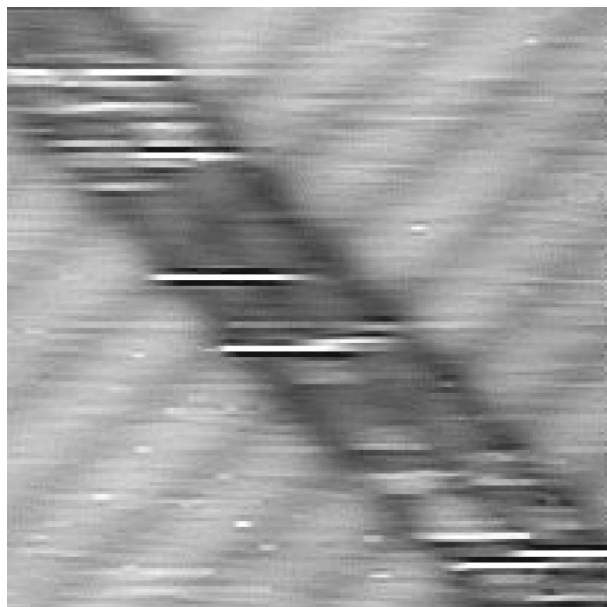


FIG. 2. A closeup image of the lines shown in Fig. 1, $40 \times 40 \text{ \AA}^2$. Bias voltage was -0.6 V . Courtesy of Dr. K. Miki.

pendicular to the silicon dimer rows, and have a width equivalent to three silicon dimers ($\sim 10 \text{ \AA}$). The internal structure visible in STM shows two features similar to silicon dimers, in phase with the dimer rows. In Fig. 2, the lines appear darker than the surrounding surface, while at higher voltages (for instance, in Fig. 1) they appear brighter. This suggests that geometrically they are at the same level as the silicon dimers, while electronically they have a larger band gap.

From the STM images, four structures have been postulated, which are illustrated in Fig. 3. The energies for the four structures are given in Table I. The STM images show two features *in line* with the silicon dimer rows in both filled and empty states, with contrast that indicates that they are almost certainly embedded in the surface. These data, along with the tight binding energies [which show that of the structures in line with silicon dimer rows, (a) is more stable by 2 eV or more per dimer], imply that structure (a) is the most likely structure.

There have recently been detailed XPD (x-ray photoelectron diffraction) measurements made of the structure of these lines,²¹ with reverse fitting to two of the structures proposed in the literature [including our structure (a)]. This confirmed that structure (a) was the structure for the line, and provided measurements of various structural parameters. These are given in Table II, along with the corresponding values as calculated using our tight binding parametrization, and recent, more detailed measurements. The good agreement seen, coupled with the absolute energies and the STM images, indicates that structure (a) is the correct structure, and provides strong evidence for the reliability of the tight binding parametrization.

B. Termination of the bismuth lines

The termination of these lines is of great interest, both from a structural point of view, and for understanding growth processes. In STM images,^{1,2} the lines embedded in

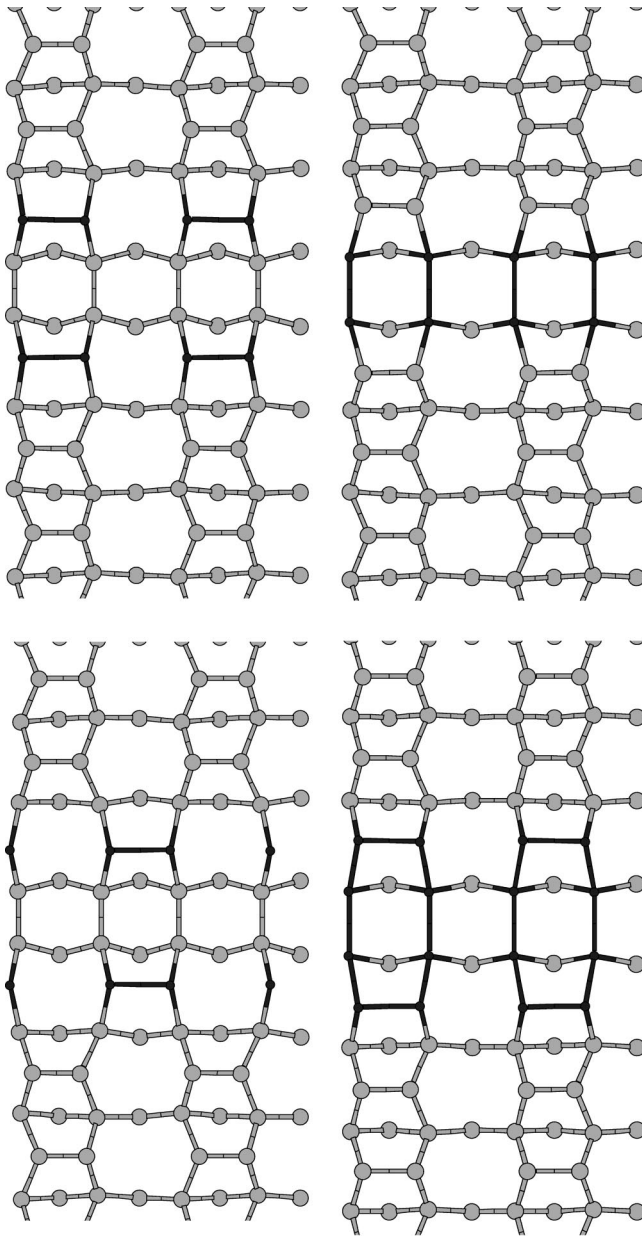


FIG. 3. Atomic positions calculated using tight binding for the proposed candidate structures for the bismuth lines. Light atoms are silicon, while dark atoms are bismuth. Only the first three layers of the unit cells are shown for clarity.

the surface are terminated either in pure silicon, or by a defect three dimers long and two rows wide ($2 \times 3DV$). Calculations to test the stabilities of these terminations (relative to an infinite line) used unit cells consisting of three dimer

TABLE II. Comparison between line structure deduced from XPD measurements and calculated from tight binding.

Parameter	Tight binding (\AA)	Expt. (\AA) (Ref. 21)
Moved in	0.48	0.3 ± 0.2
Above surface	0.57	0.7 ± 0.3
Bi-Bi bond	2.89	3.0 ± 0.3

rows of line, two dimer rows of “termination” (i.e., either $2 \times 3DV$ or pure silicon), and three dimer rows of pure silicon to provide isolation in the periodic supercell. Thus in one case the line was terminated at both ends with pure silicon, and in the other with pure silicon and two $3DV$'s.

Due to the high degree of isolation between dimer rows on Si(001), these separations were found to be sufficient to provide isolation (and provided a compromise between accuracy and computational efficiency). The calculations indicated that the terminations in pure silicon and with a pair of $3DV$'s were both slightly worse than an infinite line (although the energies are extremely small: 0.01 eV for Si and 0.20 eV for the $2 \times 3DV$), while termination with a single $3DV$ was not energetically favorable (0.99 eV worse than the perfect line). These stabilities may well be relevant for a growth mechanism; however, further experimental and theoretical work is needed before any definite conclusions can be drawn.

C. Perfection of the bismuth lines

It is observed experimentally^{1,2} that the lines show an extraordinary degree of perfection—neither kink nor defect has ever been seen in hundreds of images of lines, many of which were over 200 nm in length. It is important to determine whether this perfection arises from kinetic or thermodynamic effects.

The defect energy can be found rather simply, by removing a Bi dimer from a line segment in a supercell. The calculated energy for this in a six-dimer supercell was at least 1.1 eV less stable than a nondefective line (with the extra bismuth dimer assumed to have been placed in a line segment elsewhere on the surface); calculating the energy of a six-dimer supercell with the extra Bi dimer on the surface and adjacent to the line (as would be required were a Bi to diffuse out of the surface to create a defect in a perfect line) gave an energy 2.6 eV less stable than the perfect line. There are thus certainly strong thermodynamic reasons for the lack of defects in the line, either during formation or during annealing, and quite probably strong kinetic reasons (which would present a high barrier to diffusion out of the line).

TABLE I. The excess surface energy plus bismuth adsorption energy per Bi dimer for various possible structures of the nanolines. The different structures are illustrated, in the same order, in Fig. 3 (going from left to right and then top to bottom).

Structure	Energy (eV/dimer)
(a) Bi around a 1DV	-11.705
(b) 1DV with Bi atoms in second layer	-9.143
(c) Bi around a 1DV (Bi out of phase)	-11.659
(d) Bi around a 1DV with Bi atoms in second layer	-7.797

TABLE III. The tight binding parameters for Bi-Bi interactions.

E_s	E_p	$h_{ss\sigma}$	$h_{sp\sigma}$	$h_{pp\sigma}$	$h_{pp\pi}$	r_0	n	m	ϕ_0
-15.3	-5.87	-1.118	1.469	2.587	-0.647	3.09	3.529	6.528	2.647

A calculation of kinking energy shows that there is little change in overall energy: taking a supercell consisting of only two dimer rows, and displacing one row with respect to the other (thus creating a “maximally” kinked line), was only 0.1 eV less stable than the unkinked line. Calculations of a more isolated kink (in a six-dimer supercell, with half of the cell displaced by one dimer with respect to the other half) showed an even smaller value for the kink energy. These results are not surprising—there is a large degree of isolation between Si(001) dimer rows. So there is no equilibrium thermodynamic reason for the lack of kinks.

Kinetically, there would need to be two mechanisms at work: one to ensure that the line *formed* straight, and another to ensure that it *remained* straight after formation. Formation of the line will be addressed in later work (though they are certainly observed to form straight¹); here we consider mechanisms required to kink the line once formed.

The limiting factor in kinking is the movement of the Bi dimers. There are three possible precursors to this: diffusion of a Bi dimer out of the line onto the surface; diffusion of a Bi dimer across the line (so that there are two Bi dimers adjacent); and exchange of the Bi dimer with second-layer silicon atoms [so that the defect in the middle of the line diffuses in the standard manner²² for a 1DV on Si(001)]. We will consider each of these in turn.

The first is ruled out by the calculation performed for the defect: the energy required to move a Bi dimer out of the line and onto the surface is *at least* 2.6 eV. The second mechanism is hard to address directly, but a calculation of a six-dimer row supercell with one row in which the two Bi dimers were adjacent (so that the 1DV had moved one dimer) showed that this arrangement is 0.55 eV higher in energy than the perfect line. Whatever the barrier to diffusion across the defect (which is likely to be rather high, as the bonds between second-layer atoms forming the defect will need to be broken), this energy difference will lead to a large population imbalance between the perfect line segment and this precursor to kinking. Any further steps required to kink the line will thus be competing with the drive to return to the perfect line, and will be highly unlikely. The third mechanism can be ruled out by considering the stability of the proposed line structure (mentioned above, and given in Table I) that involves Bi atoms in the second layer: this is 5.5 eV higher in energy than the Bi line structure found above, ruling it out as a possible precursor mechanism. So we see that there are strong thermodynamic reasons for the nanoline to remain straight once it has formed, and have clear experimental evidence that it forms straight.¹

IV. CONCLUSIONS

We have described tight binding modeling of the structure and perfection of Bi nanolines in the Si(001) surface, and found that our calculated structure is in good agreement with all available experimental data. We have explored the per-

fection of the lines and reasons for this, identifying the causes for the lines remaining atomically perfect and perfectly straight after their formation. The tight binding parametrization created for modeling this problem has been described and shown to be reliable.

ACKNOWLEDGMENTS

D.R.B. is grateful to Dr. J. H. G. Owen, Dr. K. Miki, Professor D. G. Pettifor, Professor G. A. D. Briggs, Dr. C. M. Goringe, Dr. M. Fearn, Dr. A. P. Horsfield, and Dr. H. Fujitani for useful and provoking discussions, and was supported by the EPSRC.

APPENDIX A: FITTING Si-Bi AND Bi-Bi BONDING

The creation of a silicon-bismuth and bismuth-bismuth parametrization presented a number of challenges: Bi is sufficiently large that the outermost valence electrons achieve speeds through the core that make relativistic corrections necessary; there is no *AB* Si-Bi compound, making the fitting of electronic parameters to an experimental band structure impossible; and Bi in its native state is a semimetal in an arseniclike structure, with puckered graphitic sheets which are stacked sufficiently close together that the coordination is almost sixfold (which means that fitting to a tetrahedral bonding environment is hard).

The E_s and E_p levels of Bi, along with the hopping parameters, were taken from Harrison.²³ The effect on the E_s and E_p levels of relativistic corrections has been taken from a full, relativistic solution of the Dirac equation for the Bi atom, along with the offset of the Bi E_s level from the Si E_s level. This set of parameters is given in Table III. As is rather common and effective (following Chadi²⁴), the Si-Bi hopping parameters were taken as the geometric mean of the Si-Si and Bi-Bi parameters (these are given in Table IV).

The scaling for the Bi-Bi bonds and the Si-Bi bonds is again hard to fit. The following simple form has been used for the scaling of the hopping parameters:

$$h_{ll'm}(r) = h_{ll'm} \left(\frac{r_0}{r} \right)^n, \quad (\text{A1})$$

and the equivalent used for the repulsive potential [$\phi(r) = \phi_0(r_0/r)^m$]. An initial, crude estimate of the Bi-Bi bond length in tetrahedral form can be made by assuming that the ratio of bond lengths for Bi in the fcc and diamond phases will be the same as for silicon; if this ratio is applied to the

TABLE IV. The tight binding parameters for the Si-Bi interaction.

$h_{ss\sigma}$	$h_{sp\sigma}$	$h_{pp\sigma}$	$h_{pp\pi}$	r_0	n	m	ϕ_0
-1.472	1.601	2.809	-0.834	2.75	2.547	4.952	3.1187

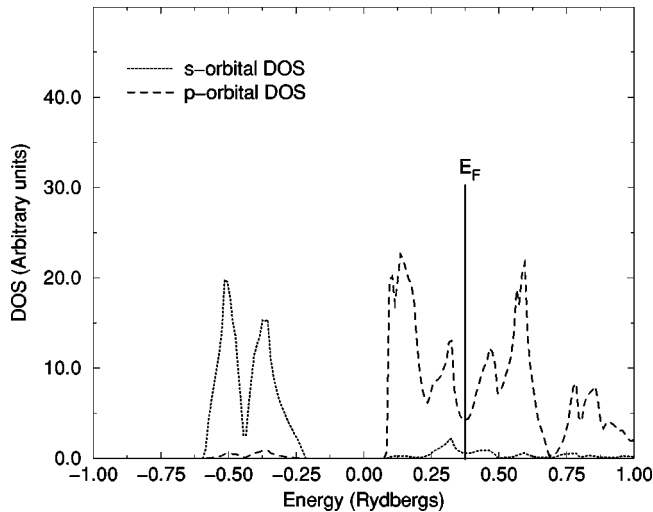


FIG. 4. The density of states (DOS) for a fictitious diamond-structure Bi cell, calculated using FLAPW.

Bi bulk bond length, the result can be taken as the Bi diamond structure bond length. The Si-Bi bond length can also be taken as the geometric mean of Si-Si and Bi-Bi.

However, this is only an extremely crude estimate, and a better fit must be constructed. Binding energy curves for Bi in tetrahedral form and zinc-blende SiBi were calculated using a full-potential linearized augmented plane wave (FLAPW) code and the tight binding scaling parameters and repulsive potentials were fitted to these. The most interesting feature of this fitting is that the bond lengths derived from these calculations were very much larger than those predicted from the simple prescription given above (3.09 Å rather than 2.52 Å). The reason for this can be seen in the local density of states for tetrahedral Bi shown in Fig. 4, where the Bi *s* band is clearly about 10 eV below the Fermi level, and is thus forming a filled, stable lone pair state, and making Bi fundamentally *p*-valent; thus the tetrahedral bonding environment will be much worse, relatively speaking, for Bi than a fcc environment would be for Si, making the bond lengths longer than anticipated.

The Bi-Bi bonding in the tetrahedral structure cannot really be tested, except through comparison of calculated surface energies with *ab initio* results; however, the robustness

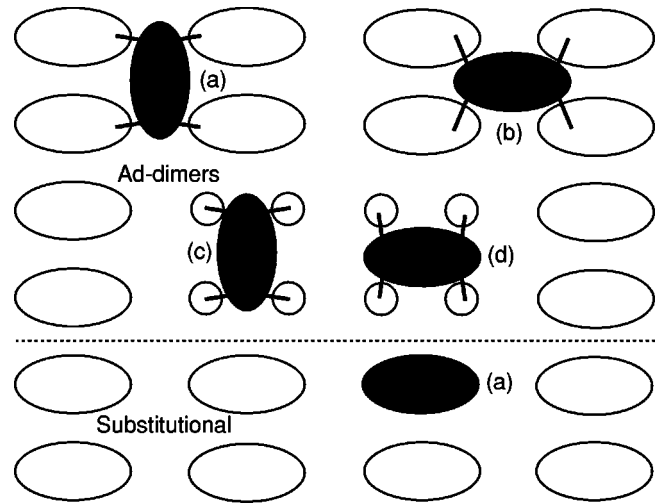


FIG. 5. A schematic diagram, showing the possible adsorption sites for Bi ad-dimers and substitutional features. Letters refer to the appropriate areas in Table V.

and transferability can be investigated by modeling the native bismuth structure, or at least a puckered sheet of bismuth, which is extremely close to the native structure. The simulation yielded a cell with nearest neighbor spacing of 3.09 (compared to 3.10 in reality) and puckering angles of 100°, compared to 90° in reality. It seems that the Bi-Bi bonding is remarkably well described.

The Si-Bi bonding, and further aspects of Bi-Bi bonding, can be investigated by considering bonding on the Si(001) surface and comparing both to experiment and more accurate *ab initio* calculations. The results of such calculations are given in the next section, and show that the parametrization is very effective for Bi dimers on and in Si(001).

APPENDIX B: STABLE STRUCTURES FOR BISMUTH DIMERS ON THE Si(001) SURFACE

The first task in investigating the behavior of bismuth on Si(001), and particularly in investigating the complex structures seen in STM, is to identify the lowest energy sites on the surface for Bi dimers. We have chosen this system as a

TABLE V. Comparison between tight binding and *ab initio* energies and bond lengths for Bi dimers in various positions on the Si(001) surface. Energies given are Bi adsorption energy plus excess surface energy per Bi atom. The Bi dimer bond length is denoted by $h(\text{Bi-Bi})$. The positions are indicated schematically in Fig. 5.

Structure	Energy (eV)	δE	<i>ab initio</i> δE	$h(\text{Bi-Bi})$ (Å)	<i>ab initio</i> $h(\text{Bi-Bi})$ (Å)
Ad-dimers					
Trench (epi) (a)	-5.51	0.23	1.11	2.88	2.96
Trench (non) (b)	-5.19	0.88	0.82	2.98	3.13
Row (epi) (c)	-5.63	0.00	0.00	2.86	2.96
Row (non) (d)	-5.44	0.38	0.51	2.89	2.96
Substitutional					
Dimer (subs) (a)	-5.75	-0.12	0.07	2.91	2.99

stringent test of the Bi-Bi and Bi-Si parametrization, and have calculated energies and structures for Bi dimers on (and in) the Si(001) surface with both tight binding and an *ab initio* electronic structure technique. As described in Sec. II, we have chosen to compare the excess surface energy (compared to a clean, perfect silicon surface) *plus* the Bi adsorption energy per Bi atom.

The *ab initio* calculations were done using the plane wave pseudopotential density functional code CASTEP.²⁵ The unit cell used was two dimers long and two dimer rows wide. It was five layers deep, with the bottom layer fixed in bulklike positions and terminated in hydrogen. Ultrasoft pseudopotentials were used with a plane wave cutoff of 250 eV and four special points in the Brillouin zone; these parameters are

sufficient for energy difference and force convergence.

The energies and Bi-Bi dimer lengths for a variety of structures (illustrated in Fig. 5) are given in Table V. With the exception of the epitaxially oriented trench dimer (i.e., with the dimer rotated by 90° relative to the underlying dimer rows), the tight binding calculations reproduce the trends in the *ab initio* calculations rather well, although the Bi-Bi bonds are perhaps a little short. Both tight binding and *ab initio* calculations predict that the Bi dimer will be most stable on top of the dimer rows, in an epitaxial orientation, as observed by STM.^{6,7} Having fitted the parametrization to a rather different environment, this agreement with *ab initio* calculations gives us confidence in using this parametrization in modeling Bi dimers on and in Si(001).

*Email address: david.bowler@ucl.ac.uk

¹K. Miki, J. H. G. Owen, D. R. Bowler, G. A. D. Briggs, and K. Sakamoto, Surf. Sci. **421**, 397 (1999).

²K. Miki, D. R. Bowler, J. H. G. Owen, G. A. D. Briggs, and K. Sakamoto, Phys. Rev. B **59**, 14 868 (1999).

³M. Copel, C. Reuter, E. Kaxiras, and R. M. Tromp, Phys. Rev. Lett. **63**, 632 (1989).

⁴K. Fujita, S. Fukatsu, H. Yaguchi, T. Igarashi, Y. Shiraki, and R. Ito, Jpn. J. Appl. Phys., Part 2 **29**, L1981 (1990).

⁵K. Sakamoto, H. Matsuhata, K. Kyoya, K. Miki, and T. Sakamoto, Jpn. J. Appl. Phys., Part 1 **33**, 2307 (1994).

⁶H. P. Noh, C. Park, D. Jeon, K. Cho, T. Hashizume, Y. Kuk, and T. Sakurai, J. Vac. Sci. Technol. B **12**, 2097 (1994).

⁷C. Park, R. Z. Bakhtizin, T. Hashizume, and T. Sakurai, J. Vac. Sci. Technol. B **12**, 2049 (1994).

⁸G. E. Franklin, S. Tang, J. C. Woicik, M. J. Bedzyk, A. J. Freeman, and J. A. Golovchenko, Phys. Rev. B **52**, R5515 (1995).

⁹P. F. Lyman, Y. Qian, T.-L. Lee, and M. J. Bedzyk, Physica B **221**, 426 (1996).

¹⁰K.-S. Kim, Y. Takakuwa, Y. Mori, and S. Kono, Jpn. J. Appl. Phys., Part 2 **35**, L1695 (1996).

¹¹Y. L. Qian, M. J. Bedzyk, P. F. Lyman, T.-L. Lee, S. P. Tang, and A. J. Freeman, Phys. Rev. B **54**, 4424 (1996).

¹²T. Hanada and M. Kawai, Surf. Sci. **242**, 137 (1991).

¹³G. A. D. Briggs and A. J. Fisher, Surf. Sci. Rep. **33**, 1 (1999).

¹⁴C. M. Goringe, D. R. Bowler, and E. H. Hernández, Rep. Prog. Phys. **60**, 1447 (1997).

¹⁵A. P. Sutton, M. W. Finnis, Y. Ohta, and D. G. Pettifor, J. Phys. C **21**, 35 (1988).

¹⁶D. R. Bowler, M. Fearn, C. M. Goringe, A. P. Horsfield, and D. G. Pettifor, J. Phys.: Condens. Matter **10**, 3719 (1998).

¹⁷Normal diagonalization or iterative minimization techniques have an effort that scales with the cube of the number of atoms. See, for instance, S. Goedecker, Rev. Mod. Phys. **71**, 1085 (1999).

¹⁸C. M. Goringe, D. Phil. thesis, Oxford University, 1995.

¹⁹X.-P. Li, R. W. Nunes, and D. Vanderbilt, Phys. Rev. B **47**, 10 891 (1993).

²⁰D. R. Bowler, M. Aoki, C. M. Goringe, A. P. Horsfield, and D. G. Pettifor, Modell. Simul. Mater. Sci. Eng. **5**, 199 (1997).

²¹M. Shimomura, K. Miki, T. Abukoura, and S. Kono, Surf. Sci. **447**, L169 (2000).

²²N. Kitamura, M. G. Lagally, and M. B. Webb, Phys. Rev. Lett. **71**, 2802 (1993); T. Yamasaki, T. Uda, and K. Terakura, *ibid.* **76**, 2949 (1996).

²³W. A. Harrison, *Electronic Structure and the Properties of Solids* (Freeman, San Francisco, 1980).

²⁴D. J. Chadi, J. Vac. Sci. Technol. A **5**, 834 (1987).

²⁵M. C. Payne *et al.*, Rev. Mod. Phys. **64**, 1045 (1992); CASTEP 4.2 Academic Version, licensed under UKCP-MSI agreement, 1999.